

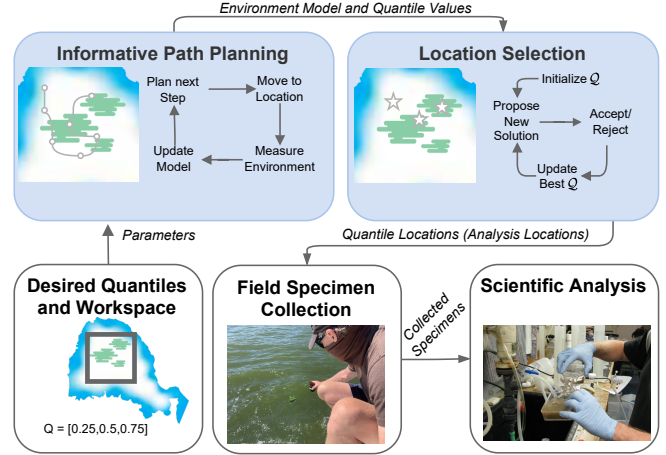
# Informative Path Planning to Estimate Quantiles for Environmental Analysis

Isabel M. Rayas Fernández<sup>†</sup>, Christopher E. Denniston<sup>†</sup>, David A. Caron, Gaurav S. Sukhatme<sup>‡</sup>

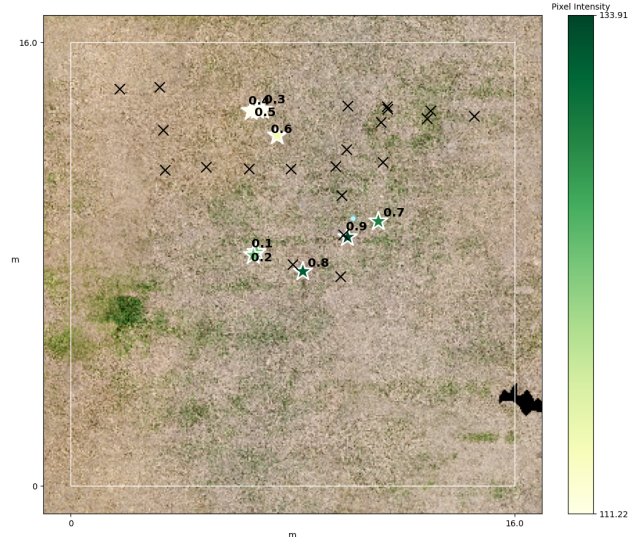
**Abstract**—Scientists interested in studying natural phenomena often take physical specimens from locations in the environment for later analysis. These analysis locations are typically specified by expert heuristics. Instead, we propose to choose locations for scientific analysis by using a robot to perform an informative path planning survey. The survey results in a list of locations that correspond to the quantile values of the phenomenon of interest. We develop a robot planner using novel objective functions to improve the estimates of the quantile values over time and an approach to find locations which correspond to the quantile values. We test our approach in four different environments using previously collected aquatic data and validate it in a field trial. Our proposed approach to estimate quantiles has a 10.2% mean reduction in median error when compared to a baseline approach which attempts to maximize spatial coverage. Additionally, when localizing these values in the environment, we see a 15.7% mean reduction in median error when using cross-entropy with our loss function compared to a baseline.

## I. INTRODUCTION

In order to understand biological phenomena, scientists take a small number of physical specimens for later analyses to characterize the biological community and the contextual environmental conditions at the site. A marine biologist may capture water in a container or filter media at a location for later analysis, and an agricultural scientist may capture a small portion of a plant. Scientists later analyze these captured portions of the environment in a detailed laboratory setting. It is often expensive to collect these physical specimens as the scientist must go to the location and use a physical reagent, such as a container or filter media, which are limited in the field. Traditionally, expert heuristics underpin the selection of locations for scientific analysis. These expert heuristics generally attempt to spread out the analysis locations in the phenomena of interest in order to take specimens with differing concentrations for characterization of heterogeneity. In contrast, we propose performing an adaptive robotic survey to find locations of interest for scientific analysis. To specify these locations, we propose



(a) **Full system.** First, the parameters for the robotic survey are chosen, such as the bounds of the area and the quantiles for specimen collection. The robot performs informative path planning, creating an environment model and an estimate of the quantile values. The quantile locations are then selected which correspond with the estimated quantile values. After the quantile locations are chosen, humans go to them to collect field specimens which they later analyze in a laboratory setting. This work focuses on the steps shown in the blue shaded boxes.



(b) **Visualization of a field trial modeling a crop health task.** Crosses are locations where a drone took images. The drone is limited to only visit 20% of the possible locations to take images. The 9 stars show locations suggested by the drone using cross-entropy optimization to sample for the deciles. The measurement of interest is the amount of green in each pixel. The experiment was geofenced within the white border.

Fig. 1

<sup>†</sup> Equal contribution.

All authors are with the University of Southern California.  
rayas, cdennist, dcaron, gaurav@usc.edu

<sup>‡</sup> G.S. Sukhatme holds concurrent appointments as a Professor at USC and as an Amazon Scholar. This paper describes work performed at USC and is not associated with Amazon.

This work was supported in part by the Southern California Coastal Water Research Project Authority under prime funding from the California State Water Resources Control Board on agreement number 19-003-150 and in part by USDA/NIFA award 2017-67007-26154.

This material is based upon work supported by the National Science Foundation Graduate Research Fellowship Program under Grant No. DGE-1842487. Any opinions, findings, and conclusions or recommendations expressed in this material are those of the author(s) and do not necessarily reflect the views of the National Science Foundation.

calculating the quantiles of the distribution of interest so that scientists can capture specimens at varied locations in the environment based on differing values of some phenomenon of interest to them. For instance, if a marine biologist is interested in taking 9 physical water specimens that are spread over a range of chlorophyll concentrations, they may choose to use the deciles of the concentration. If only a small number of locations can be analyzed and the upper extrema values are of interest, they may choose to perform analysis at the locations of the (0.90, 0.95, 0.99) quantiles. The quantiles of interest are a flexible way for a human to describe the objective of specimen collection that is largely invariant to the exact phenomena being measured.

Our goal is to select locations for detailed analysis by scientists in two steps. First we use a robot to perform an adaptive survey, and then find locations to suggest for specimen collection based on the measurements it takes. Specifically, we aim to find the desired quantile values of the measurement distribution by adaptively selecting robot measurement locations that maximize an objective function designed to estimate quantile values, and then we produce suggested locations for specimen collection that are likely to contain the estimated quantile values.

We develop our method using an informative path planning formulation and show that it outperforms entropy- and sequential Bayesian optimization-based objective baselines. Our contributions are:

- A planner with custom objective functions for adaptively increasing the quality of estimated quantiles;
- A method to select spatial locations which have the values estimated for the quantiles;
- Quantitative evaluation of our method on point and camera sensors with previously collected aquatic datasets;
- A demonstration of our method on a robot in a real-world crop health estimation task.

## II. RELATED WORK

Informative path planning has a long history in use for studying biological phenomena [1], [2]. Often, the objective in informative path planning is to generate good coverage of a distributed phenomenon using an information theoretic objective such as entropy [3] or mutual information [4]. Our work differs from these works by instead focusing on improving estimates for specific quantiles instead of broad understanding of the spatial makeup of a distribution.

Other common objectives include finding the highest concentration location [5] or measuring near hotspots [6]. Sequential Bayesian optimization objectives are used to locate extreme values or areas of high concentration and have shown success in doing so in simulation and in real field scenarios [5], [7], [8]. These specialized objective functions are typically tuned to locate a single specific point, often the extrema, by increasing the quality of the estimate of the underlying concentration. Our work differs from work which seeks to find these maxima by instead finding values at different quantiles of the distribution of interest.

Selecting physical specimen collection locations using adaptive surveys have typically focused on finding high-concentration areas from which to measure and perform the specimen collection onboard the robot, or by a following robot [9], [10]. Our work differs from works which perform specimen collection onboard a robot as we do not seek to only find maximal concentration areas.

Formulating informative path planning as a partially observable Markov decision process (POMDP) has been explored [11]; previous works have used this for finding maxima [5] and to adapt the parameters of a rollout-based POMDP solver online to improve its efficiency for informative path planning [2]. We use these works to formulate and solve the informative path planning problem.

Previous works have also investigated directly calculating the quantile values for distributions at points using specialized loss functions to extend the notion of uncertainty in Gaussian processes, but these do not directly transfer to our setting because they only estimate the quantiles of a specific location [12], [13] rather than of the entire distribution.

## III. BACKGROUND

**Gaussian Processes (GPs)** are non-parametric models with uncertainty quantification which are widely used for informative path planning [5], [2], [3]. They approximate an unknown function from its known outputs by computing the similarity between points from a kernel function, in our case the squared exponential kernel [14]. GPs have been used to represent the belief distribution from observations in POMDP formulations of sequential Bayesian optimization and informative path planning [11], [5], [2]. In this work we use a GP as the environment model to estimate the value  $\mu(x)$  and variance  $\sigma^2(x)$  at a specific location  $x$ .

**Online Informative Path Planning** consists of alternating between planning and taking an action, which usually corresponds to moving and measuring a value at the new location. A plan described by a partial trajectory  $p$  is created to maximize some objective function  $f$  over the measured locations  $X$  and measured values  $Y$ . The combined plan  $P$  is the concatenation of partial trajectories  $p$ . The plan and act steps are iterated until the cost  $c(P)$  exceeds some predefined budget. Formally, this can be described by  $P^* = \operatorname{argmax}_{P \in \Phi} f(P) \mid c(P) \leq B$ , where  $\Phi$  is the space of full trajectories, and  $P^*$  is the optimal trajectory [15], [2].

**Informative Path Planning as a Partially Observable Markov Decision Process (POMDP)** provides a formulation for planning for taking measurements. POMDPs are a framework that can determine optimal actions when the environment is not fully observable or there is uncertainty in the environment. Using observations as measurements from the environment and a GP to represent the belief distribution, sequential Bayesian optimization can be formulated as a Bayesian search game [11]. Measurements from the environment  $y_t = GT(x_t)$  constitute observations which are partially observable components of the overall environment  $GT$ . To adapt the Bayesian search game formulation to informative path planning, the belief state is augmented with

POMDP	Informative Path Planning
States	Robot position $g_t$ , Underlying unknown function $GT$
Actions	Neighboring search points
Observations	Robot position $g_t$ , Measured location(s) $x_t = o(g_t)$ Measured value(s) $y_t = GT(x_t)$
Belief	$GP(\mathbf{X}_{0:t}, \mathbf{Y}_{0:t})$
Rewards	$f(x_t)$

TABLE I: **Informative Path Planning as a POMDP.** After [11], [2].

the state of the robot  $g_t$  and the actions the planner is allowed to take are restricted to local movements which are feasible for the robot [5]. A complete description of the POMDP for informative path planning can be seen in Table I. We approximately solve this POMDP to select actions to take measurements for maximizing the objective function.

**Estimation of Quantiles and Quantile Standard Error** has been proposed using statistical techniques. We estimate the quantile value from measurements using  $\tilde{v} = x_{[h]} + (h - [h])(x_{[h]} - x_{[h]})$  where  $h = (n - 1)q + 1$ ,  $n$  is the number of measurements, and  $q$  is the quantile (Equation 7 in [16])<sup>1</sup>. The standard error of a quantile estimate is a measure of the uncertainty of that quantile estimate, and is typically used in the estimate of confidence intervals of a quantile value. Given a probability density function  $p$ , the standard error of the  $q$ th quantile is  $\frac{\sqrt{q(1-q)}}{\sqrt{np(\tilde{v})}}$ . This method requires  $p$ , which is typically not known. To estimate  $p$  from samples, a density estimate can be constructed [17]. Here we use a Gaussian Kernel density estimator to estimate the standard error when planning. Other estimation methods include the Maritz-Jarrett method [18], and the bootstrap or jackknife methods which involve calculating the quantiles over repeatedly sampled subsets of the data. These last two methods can be slow for large datasets and require many iterations to converge.

**Continuous Non-Convex Gradient-Free Optimization** is used to solve general black-box optimization problems. We use these methods to select the analysis locations once the informative path planning survey is completed.

One common approach is the cross-entropy (CE) method [19]. CE works by maintaining an estimate about the distribution of good solutions, and iteratively updating the distribution parameters based on the quality of the solutions sampled at each step, where the quality is determined via some function of the solution configuration. More precisely, a prior  $Pr$  and a posterior  $Po$  set of samples are maintained.  $Po$  contains  $n$  configurations sampled from a Gaussian distribution defined by parameters  $\vec{\mu}$  and  $\vec{\sigma}$ .  $\vec{\mu}$  and  $\vec{\sigma}$  are computed from  $Pr$ , which is the best  $\eta\%$  configurations from  $Po$ . This continues iteratively for a fixed number of iterations or until a stopping criterion is met. By taking these iterative steps, CE minimizes the cross-entropy between the maintained distribution and a target distribution [19].

Another popular optimization method is simulated annealing (SA) [20], an iterative improvement algorithm inspired by statistical mechanics. SA optimizes an energy function

similar to a loss function in other optimization schemes, as configurations with lower energy are preferred. SA begins with a temperature  $T = T_{\max}$ . At each iteration,  $T$  is decreased exponentially, and the configuration is slightly perturbed randomly. The perturbed state is either accepted or rejected probabilistically based on its energy and  $T$ . The algorithm terminates when  $T$  reaches a given threshold.

Bayesian optimization (B) is a popular method for selecting parameters for difficult optimization problems such as hyperparameter selection [21]. BO is similar to informative path planning and sequential Bayesian optimization [5] in that these methods build a model using a Gaussian process and select points which maximally improve this model. In pure BO the optimizer is allowed to select any points in a defined boundary, as opposed to informative path planning and sequential Bayesian optimization, where the robot can only select points it can locally travel to. BO uses acquisition functions, such as expected improvement, and iteratively selects the best point to sample from [22], [23].

#### IV. FORMULATION

We use a grid-based representation of the planning space,  $G^\#$ , which defines the set of locations that the robot could visit. For a robot that moves in  $\mathbb{R}^d$ ,  $G^\# \subset \mathbb{R}^d$ .  $X^\#$  is the set of locations the robot could measure. If the robot sensor has finer resolution, than  $G^\#$ , then  $|X^\#| > |G^\#|$ . This is true e.g. when the robot uses a camera sensor or takes measurements while traversing between grid points. We define  $X$  as the locations the robot has already measured and  $Y^\#$  and  $Y$  as the values at all possible measured locations, and the values the robot has measured, respectively.

We define the ground truth quantile values as  $V = \text{quantiles}(Y^\#, Q)$  where  $\text{quantiles}$  is the function described in Section III which computes the values  $V$  of the quantiles  $Q$  of a set of measurements. To define the robot's estimated quantile values, we compute  $\tilde{V} = \text{quantiles}(\mu(X^\#), Q)$  that is, the quantile values of the predicted values from the robot's current GP for all locations the robot could sense. This is done to prevent the number of measurements from which the quantile values are estimated from changing as the robot explores (instead of, e.g. using  $\mu(X)$ ). By doing this, we ensure we always estimate the quantiles across the entire measurable area. To assess estimation accuracy, we compute the error using  $RMSE(\tilde{V}, V)$ . During planning, we aim to minimize this error by taking actions which maximize an objective function  $f$  that minimizes the error in the quantile value estimate.

To suggest locations for the quantile values, we aim to find a set of  $|Q|$  locations  $Q$  in the continuous space whose values at those locations are equal to the quantile ground-truth values. A set of locations is defined as  $Q \in Q^\#$  where  $Q^\# \subset \mathbb{R}^{d \times |Q|}$  and  $Q^\#$  is continuous over the space of  $G^\#$ . In practice, the robot only has access to  $\tilde{V}$  (not  $V$ ) during the selection process, so the problem of finding the estimated quantile spatial locations  $\tilde{Q}$  can be stated as shown in eq. (1)

<sup>1</sup>This is the default in the `numpy` Python package.

with some selection loss function  $l_s$ , discussed later.

$$\tilde{Q} = \arg \min_{Q' \subset Q^\#} l_s(\tilde{V}, Q') \quad (1)$$

## V. APPROACH

Figure 1a illustrates our method. We separate our approach into two steps, the survey and the suggestion of points. When performing the survey using informative path planning (Section V-A), the robot takes measurements of the environment to improve its model of the environment and estimate of the quantiles. After the survey has concluded, location selection (Section V-B) performs estimation of the locations for scientists to visit to perform specimen collection.

### A. Informative Path Planning

To plan which locations to sample, the robot uses the POMDP formulation of informative path planning. In order to generate a policy, we use the partially observable Monte Carlo planner (POMCP) [24]. POMCP uses Monte Carlo tree search to create a policy tree. To expand the tree and estimate rewards, the tree is traversed until a leaf node is reached. From the leaf node, a rollout of a random policy is performed to estimate the reward conditioned on that action. For each rollout a random policy is executed until the discounted reward is smaller than some value  $\epsilon$ . We modify the rollout reward to be fixed horizon which gives a reward of zero once a certain number of random policy steps are taken. We adopt the t-test heuristic for taking multiple steps from a POMCP plan for informative path planning to improve performance of the planner with fewer rollouts [2]. Because the observations  $GT(x)$  for unseen locations are not known during planning, the predicted mean from the GP conditioned on the previous observations is used [5].

**Objective Functions for Quantile Estimation** We develop two novel objective functions to improve the quality of planning for estimating quantile values. Both functions compare a measure of the quality of the quantiles estimated by the GP before and after adding the measurement to the GP. For both functions, we include an exploration term  $c_{plan}\sigma^2(x_i)$ , inspired by the upper confidence bound objective function [5], where  $c_{plan}$  is a chosen constant. For both objective functions,  $GP_{i-1} = GP(\mathbf{X}_{0:i-1}, \mathbf{Y}_{0:i-1}; \theta)$  is a GP conditioned on the points before measuring a proposed value, and  $GP_i = GP(\mathbf{X}_{0:i-1} \cup \mathbf{X}_i, \mathbf{Y}_{0:i-1} \cup \mathbf{Y}_i; \theta)$  is a GP conditioned on the previous and proposed measurements, where  $\theta$  are GP parameters and  $\mathbf{Y}_i = GP_{i-1}(\mathbf{X}_i)$ . For both proposed objective functions we use eq. (2):

$$f(x_i) = \frac{\delta}{|Q|} + c_{plan}\sigma^2(x_i), \quad (2)$$

where  $\delta$  is defined by the objective.

The first objective function, which we call *quantile change*, is based on the idea of seeking out values which change the estimate of the quantile values by directly comparing the estimated quantiles before and after adding the measured values to the GP. The idea behind this is that a measurement which changes the estimate of the quantiles

indicates that the quantiles are over- or under-estimated. This can be seen in in eq. (3):

$$\delta_{qc} = \|\text{quantile}(\mu_{GP_{i-1}}(\mathbf{X}^\#), Q) - \text{quantile}(\mu_{GP_i}(\mathbf{X}^\#), Q)\|_1 \quad (3)$$

The second objective function we develop, which we call *quantile standard error*, is based on the change in the estimate of the standard error for the estimated quantiles. It draws from the same idea that if the uncertainty in the quantile estimate changes after observing a measured value, then it will change the estimate of the quantile values, shown in eq. (4):

$$\delta_{se} = \|se(\mu_{GP_{i-1}}(\mathbf{X}^\#), Q) - se(\mu_{GP_i}(\mathbf{X}^\#), Q)\|_1 \quad (4)$$

$se$  is an estimate of the standard error of the quantile estimate for quantiles  $Q$ .  $se$  uses a Gaussian kernel density estimate (we found it faster and more stable than the Maritz-Jarrett estimator, and considerably faster than sampling-based estimators, such as bootstrap and jackknife).

**Baseline Objective Functions** We compare against two baselines, one which maximizes spatial coverage of a phenomena and another which seeks maximal areas.

*Entropy* is a common objective function for informative path planning when only good spatial coverage of the environment is desired [3], [4], [25]. It provides a good baseline as it is often used when the specific values of the underlying concentration are unknown. Entropy is defined by rescaling the variance in the GP at the location according to eq. (5):

$$f_{en}(x_i) = \frac{1}{2} \log(2\pi e \sigma^2(x_i)) \quad (5)$$

Another objective function we compare against is *expected improvement*, which is widely used in Bayesian optimization and sequential Bayesian optimization for finding maxima [22], [23]. Expected improvement favors actions that offer the best improvement over the current maximal value, with an added exploration term  $\xi$  to encourage diverse exploration. The expected improvement objective function is defined according to eq. (6):

$$I = (\mu(x_i) - \max(\mu(\mathbf{X}^\#)) - \xi) \quad Z = \frac{I}{\sigma^2(x_i)} \quad (6)$$

$$f_{ei}(x_i) = \begin{cases} 0 & \sigma^2(x_i) = 0 \\ I\Phi(Z) + \sigma(x)\phi(Z) & \sigma^2(x_i) > 0 \end{cases}$$

where  $\Phi$  and  $\phi$  are the CDF and PDF of the normal distribution, respectively.

### B. Location Selection

Our final goal is to produce a set of  $|Q|$  locations  $Q$ , at which the concentration values will be equal to  $V$ , the values of the quantiles  $Q$ . The selection process can be done offline as it does not affect planning. Finding locations that represent  $Q$  is difficult because the objective function over arbitrary phenomena in natural environments will likely be non-convex, and in a real-world deployment, the robot will only have an estimate  $\tilde{V}$  of the  $V$  it searches for.

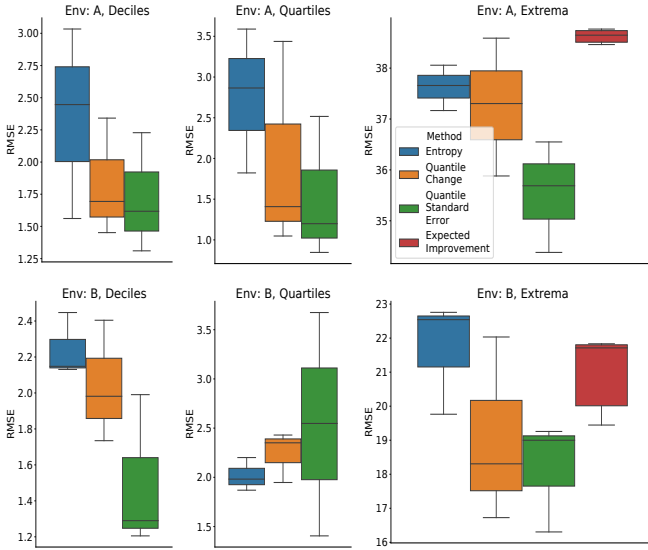


Fig. 2: **Simulated drone planning experiments with real data.** Error between ground truth quantile values and estimated quantile values in a task with a simulated drone with a camera using datasets A and B collected in Clearlake, California. Units are pixel brightness.

With the location selection problem formulation as in Equation (1), we use

$$l_s(\tilde{V}, \tilde{Q}) = \|\tilde{V} - \mu(\tilde{Q})\|_2 + c_{select}\sigma^2(\tilde{Q}), \quad (7)$$

where  $c_{select}\sigma^2(\tilde{Q})$  is an added penalty for choosing points that the GP of collected measurements is not confident about. The parameters  $c_{plan}$  and  $c_{select}$  are distinct;  $c_{plan}$  is an added exploration bonus for reducing uncertainty during the planning phase while  $c_{select}$  is an added penalty for choosing uncertain points.

The optimizer runs using  $\tilde{V}$  and returns the suggested specimen collection locations  $\tilde{Q}$ . We compare simulated annealing, cross-entropy, and Bayesian optimization methods in our experiments to determine which optimization strategy best minimizes eq. (7). A strength of these types of optimization methods is that the formulation allows for suggesting points that may be spatially far from locations the robot was able to measure if they have values closer to the quantile values of interest.

## VI. EXPERIMENTS

To evaluate our approach, we compare against baselines in two different informative path planning tasks in simulation using datasets collected in the real world.

In the first task, a drone is simulated with a virtual camera over orthomosaics (a single image produced by combining many smaller images, called orthophotos) collected of a lake using a hyperspectral sensor. The drone collects many measurements from one location, with each one being a pixel in a downsampled image. As a proxy for chlorophyll concentration, we are interested in calculating the quantiles of the pixel intensity. The drone maintains a constant altitude and moves in a 2D plane with a north-fixed yaw and makes

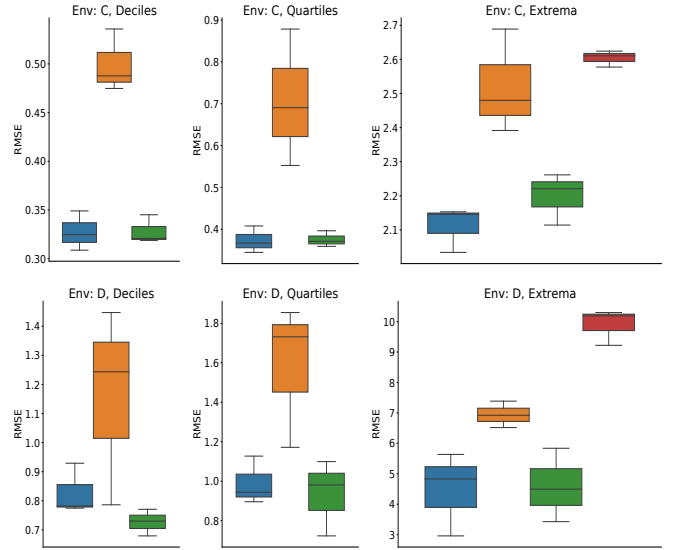


Fig. 3: **Simulated AUV planning experiments with real data.** Error between ground truth quantile values and estimated quantile values. Datasets C and D collected from a reservoir in California. Units are  $\mu g/L$  chlorophyll.

a move in either the  $x$  or  $y$  direction per step. The two orthomosaics, A and B, are taken in the same location but on different days and times.

In the second task, an autonomous underwater vehicle (AUV) explores a 3D workspace interpolated from a 3D lawnmower survey collected previously. The lawnmower survey is interpolated using a GP to  $\mathbf{X}^\#$ . At each step the AUV may move in one  $x$ ,  $y$ , or  $z$  direction. The AUV takes five evenly spaced samples when moving between locations. The two AUV surveys, C and D, are taken in the same reservoir at different times and in different areas of the lake. The AUV surveys were conducted using a chlorophyll sensor.

For each task, we compare on two different datasets (A/B, C/D) and three different quantiles: deciles (0.1, 0.2, ..., 0.8, 0.9), quartiles (0.25, 0.5, 0.75) and upper extrema (0.9, 0.95, 0.99). We choose these quantiles to demonstrate the flexibility of the objectives that our approach can handle.

### A. Informative Path Planning: Objective Functions

To compare the ability of our proposed objective functions, quantile change (eq. (3)) and quantile standard error (eq. (4)), we compare against a baseline entropy objective function (eq. (5)). For the upper extrema quantiles, we also compare against expected improvement (eq. (6)), as it is similar to a sequential Bayesian optimization based informative path planning task. In the planner, we use  $\gamma = 0.9$ , and each trial is run over 3 seeds. The objective  $c_{plan}$  parameter is set to the approximate magnitude of the rewards seen for each environment, which we found experimentally to be an adequate value. The parameters for the GPs were all found experimentally.

Overall, our results are robust across multiple experimental



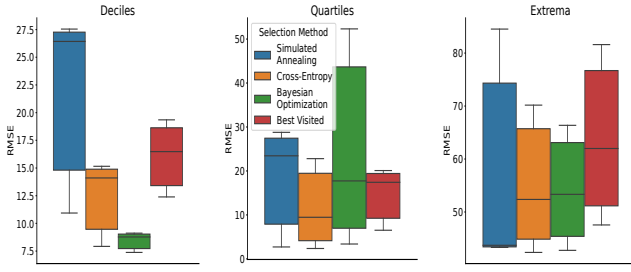


Fig. 4: **Quantile location selection results for drone experiments.** RMSE between the actual (ground truth) values at the selected locations and the corresponding actual quantile values. Units are pixel brightness.

environments as well as robot sensor types. We find that planning with the quantile standard error objective function has a 10.2% mean reduction in median error across all environments when compared to using entropy as the objective function.

1) *Drone with Camera:* For this task, the drone is allowed to take 30 simulated pictures out of a grid with about 300 positions. Each simulated picture is downsampled to 8 by 5 pixels with  $37.1^\circ$  by  $27.6^\circ$  field of view, similar to the drone used in the field trial reported in section VI-C. At each step, the drone collects  $8 \times 5 = 40$  measurements. For each trial, the GP used by the robot is seeded with 100 evenly spaced points across the workspace, as a proxy for data given by a remote sensor, such as a satellite. In the planner, 300 rollouts per step are used and the maximum planning depth is 7.

Figure 2 shows the results of planning with the proposed objective functions. Quantile change and quantile standard error outperform the baseline entropy in estimating the deciles and upper extrema. In quartiles in environment A, both proposed methods perform well, but in environment B entropy outperforms our methods. For the extrema, both methods perform better than expected improvement and entropy outperforms expected improvement in environment A. We believe this is because expected improvement only looks to improve the maximal value and does not do a good job of localizing high concentration areas instead of a single point, and focuses explicitly on this point which can cause an over estimation of the quantile values.

2) *AUV with Chlorophyll Sensor:* The AUV is simulated for 200 steps in a  $12 \times 14 \times 2$  grid. The planner uses 130 rollouts per step and a maximum depth of 10. The GP is seeded with values from 50 locations.

Figure 3 shows the results of this experiment. Quantile standard error outperforms entropy in environment C when estimating deciles and quartiles, and performs equally well as entropy in all other tasks besides estimating the extrema in environment D. Quantile change performs poorly in most tasks, and expected improvement performs poorly in estimating the extrema due to similar issues as the previous task.

### B. Location Selection

To produce suggested physical specimen collection locations, we use the optimization algorithms simulated annealing, cross-entropy, and Bayesian optimization with the results

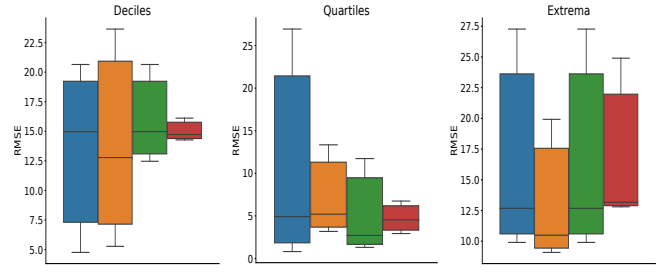


Fig. 5: **Quantile location selection results for AUV experiments.** RMSE between the actual (ground truth) values at the selected locations and the corresponding actual quantile values. Units are  $\mu g/L$  chlorophyll.

from the measurements gathered by the quantile standard error objective function on the quantile estimation task. We compute the error by  $RMSE(V, \tilde{Q}) = \|(V - GT(\tilde{Q}))\|_2$ . We set  $c_{select}$  to 15 for deciles, 200 for quartiles, and 30 for extrema. We compare these results against a Best Visited baseline which selects the location the robot took a measurement at that is closest to each quantile value, i.e. solve  $\tilde{Q}^* = \arg\min_{\tilde{Q}_{bv} \subset X} \|\tilde{V} - \mu(\tilde{Q}_{bv})\|_2$ .

For simulated annealing, we use  $T_{max} = 5$ ,  $T_{min} = 0.001$ , and cooling rate  $cr = 0.005$  which leads to approximately 1000 optimization steps, and reset to the best solution every 100 steps. We start the optimization using the solution found by the Best Visited baseline.

For Cross-Entropy, we use  $\alpha = 0.9$ ,  $\eta = 0.9$ , 50 samples per iteration, and 100 iterations.  $\alpha$  is a weighting factor on new samples, which is used to prevent premature convergence.

For Bayesian Optimization, we use the expected improvement acquisition function and initialize the GP with 50 randomly selected  $Q$ s as well as the solution found by the Best Visited baseline. We run Bayesian optimization for 100 iterations and report the best found solution.

The error between the values at the estimated quantile locations and the true quantile values for the drone and the AUV experiments can be seen in Figure 4 and Figure 5, respectively. Overall, we find that cross-entropy and Bayesian optimization produced the locations with values closest to the true quantile values. Both these methods perform a global search in the space of possible locations which indicates that global search optimizes eq. (7) more effectively. Simulated annealing had greater variability in performance. We believe this is because it is a local search method and may fail to escape local optima. Best Visited produced a good initialization point for the other methods, but was easily outperformed. We find that cross-entropy performs the best in three out of six possible scenarios. In particular, we see a 15.7% mean reduction in median error using cross-entropy with our proposed loss function compared to the Best Visited baseline across all environments when using our proposed quantile standard error optimization function for quantile estimation during exploration.

1) *Drone with Camera:* Figure 4 shows  $RMSE(V, \tilde{Q})$  for the drone experiments for each of the four point selection

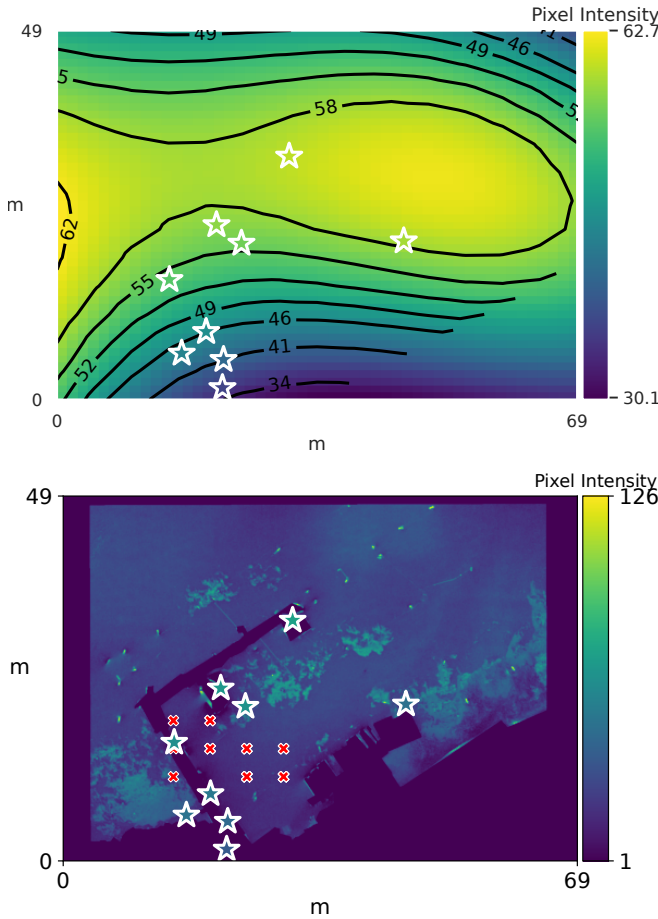


Fig. 6: **Physical locations (white stars) selected by the cross-entropy optimizer for deciles on the drone experiment.** [Top] Black lines: true quantile value contours. [Bottom] Red crosses: locations the robot visited, overlaid on the ground truth raster image.

methods. In general, the methods can find the best points when selecting for quartiles or deciles, while the upper extrema are more difficult. Because the robot is limited in the amount of environment it can explore, the upper extrema are less likely to be measured during exploration. This leads to these quantiles being more challenging to select representative points for.

Figure 6 shows results for one seed of the drone with a camera sensor when monitoring deciles. The suggested locations, shown as stars, align relatively closely with the true quantile values  $V$ , shown by the contours. This demonstrates the ability of the optimizers to produce good location suggestions to guide environmental analysis.

The bottom part of Figure 6 shows the same locations on top of the orthomosaic of what the drone could measure during exploration. This part of the figure highlights the difficulty of the problem of informative path planning for quantiles. The robot could only explore 15% of the total environment. With only partial knowledge of the distribution, the robot’s model of the phenomenon will vary based on the particular points it visited, which in turn affects the estimates

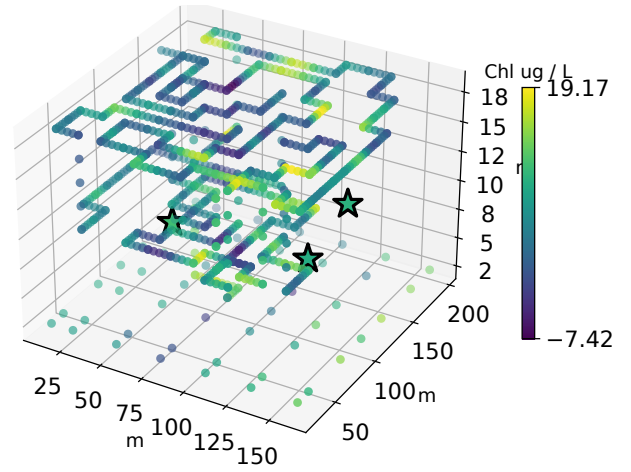


Fig. 7: **Physical locations (stars) selected by the cross-entropy optimizer for the upper extrema quantiles with an AUV using a chlorophyll point sensor.** Blue/green points are the measured locations  $X$ .

of the quantiles.

2) *AUV with Chlorophyll Sensor*: Figure 5 shows  $RMSE(V, \hat{Q})$  for the AUV experiments for each of the four point selection methods. Like in the drone experiments, the suggested locations correspond well to  $V$  produced by the planner. Here, cross-entropy performs best for both the extrema and the deciles, demonstrating the effectiveness of global search.

Figure 7 shows the suggested locations for the upper extrema for one seed. All the optimization methods, with the exception of Best Visited, suggest points that may be spatially far from locations the robot has been able to visit. This allows for points with values potentially closer to the true quantile values to be selected for scientific analysis.

### C. Field trial

In our final experiment, we demonstrate our method on a crop health monitoring task, where the objective is to estimate the deciles of the green present in each pixel of the images (we use green as a proxy for plant health). We use a commercial, off-the-shelf drone with a standard camera to take measurements of the field at a constant height of 3m. Similar to the simulated drone, the drone in this experiment moves in a 2D plane with a north-fixed yaw. The drone can take 20 pictures (planning steps) in a  $16 \times 16$  m square grid, where  $|G^\#| = 10 \times 10 = 100$  points, and each picture is downsampled to 8 by 5 pixels. For planning, we use the quantile change objective function because it performs well for camera sensors and is faster than quantile standard error.

Figure 1b shows the resulting suggested locations using cross-entropy based on the 20 steps shown that the robot took. We find that, although the robot does not explore the entire workspace due to the limitation to take pictures at only 20 locations, and in fact misses a large green area, the system is able to suggest varied locations for specimen collection along the sampled areas.

## VII. CONCLUSION

Scientists traditionally collect physical specimens at locations selected using heuristics. They later analyze these specimens in a laboratory to characterize a phenomenon of interest (e.g., the distribution of algae in the water). We propose to, instead, choose these specimen collection locations by first performing an informative path planning survey with a robot and then proposing locations which correspond to the quantiles of interest of the distribution.

To accomplish this, we propose two novel objective functions, quantile change and quantile standard error, for improving the estimates of quantile values through informative path planning. We test these in three settings: a drone with a camera sensor over lake imagery, an underwater vehicle taking chlorophyll measurements, and a field trial using a drone for a crop health monitoring task. Our objective functions perform well on these tasks and outperform information theoretic and Bayesian optimization baselines. In our experiments, our proposed quantile standard error objective function has a 10.2% mean reduction in median error when compared to using entropy as the objective function.

We also show that optimization methods like simulated annealing, cross-entropy and Bayesian optimization can select analysis locations in the environment that are representative of a set of quantiles of interest when combined with an adaptive survey for those quantiles. We find that cross-entropy using our proposed loss function outperforms a baseline of using the best measured points. In our experiments, we see a 15.7% mean reduction in median error using cross-entropy compared to the baseline across all environments when using our proposed quantile standard error optimization function.

Our approach can be used to guide physical specimen collection in real field scenarios, as demonstrated by our field trial. We also plan to incorporate our specimen collection location suggestions into a larger field campaign involving multiple scientists.

## REFERENCES

- [1] T. O. Fossum, J. Eidsvik, I. Ellingsen, M. O. Alver, G. M. Frago, G. Johnsen, R. Mendes, M. Ludvigsen, and K. Rajan, "Information-Driven Robotic Sampling in the Coastal Ocean," *Journal of Field Robotics*, vol. 35, no. 7, pp. 1101–1121, 2018.
- [2] C. E. Denniston, G. Salhotra, D. A. Caron, and G. S. Sukhatme, "Adaptive Sampling using POMDPs with Domain-Specific Considerations," in *2020 International Conference on Robotics and Automation*, Oct 2020.
- [3] S. Kemna, O. Kroemer, and G. S. Sukhatme, "Pilot Surveys for Adaptive Informative Sampling," in *2018 IEEE International Conference on Robotics and Automation (ICRA)*, May 2018, pp. 6417–6424, iSSN: 2577-087X.
- [4] C. Guestrin, A. Krause, and A. P. Singh, "Near-optimal sensor placements in Gaussian processes," in *Proceedings of the 22nd international conference on Machine learning - ICML '05*. Bonn, Germany: ACM Press, 2005, pp. 265–272.
- [5] R. Marchant, F. Ramos, and S. Sanner, "Sequential Bayesian optimization for spatial-temporal monitoring," in *Proceedings of the Thirtieth Conference on Uncertainty in Artificial Intelligence*, ser. UAI'14. Arlington, Virginia, USA: AUAI Press, Jul. 2014, pp. 553–562.
- [6] S. McCammon and G. A. Hollinger, "Topological Hotspot Identification for Informative Path Planning with a Marine Robot," in *2018 IEEE International Conference on Robotics and Automation (ICRA)*. IEEE, May 2018, pp. 1–9.
- [7] A. Blanchard and T. Sapsis, "Informative Path Planning for Extreme Anomaly Detection in Environment Exploration and Monitoring," *arXiv:2005.10040 [cs, stat]*, Apr. 2021, arXiv: 2005.10040.
- [8] J. R. Souza, R. Marchant, L. Ott, D. F. Wolf, and F. Ramos, "Bayesian optimisation for active perception and smooth navigation," in *2014 IEEE International Conference on Robotics and Automation (ICRA)*, May 2014, pp. 4081–4087, iSSN: 1050-4729.
- [9] J. Das, F. Py, J. B. Harvey, J. P. Ryan, A. Gellene, R. Graham, D. A. Caron, K. Rajan, and G. S. Sukhatme, "Data-driven robotic sampling for marine ecosystem monitoring," *The International Journal of Robotics Research*, vol. 34, no. 12, pp. 1435–1452, Oct. 2015, publisher: SAGE PublicationsSage UK: London, England.
- [10] S. Manjanna, A. Q. Li, R. N. Smith, I. Rekleitis, and G. Dudek, "Heterogeneous multi-robot system for exploration and strategic water sampling," in *2018 IEEE International Conference on Robotics and Automation (ICRA)*, 2018, pp. 4873–4880.
- [11] M. Toussaint, "The Bayesian Search Game," in *Theory and Principled Methods for the Design of Metaheuristics*, Y. Borenstein and A. Moraglio, Eds. Berlin, Heidelberg: Springer Berlin Heidelberg, 2014, pp. 129–144, series Title: Natural Computing Series.
- [12] A. Boukouvalas, R. Barillec, and D. Cornford, "Direct Gaussian Process Quantile Regression Using Expectation Propagation," in *Proceedings of the 29th International Conference on International Conference on Machine Learning*, ser. ICML'12. Madison, WI, USA: Omnipress, 2012, p. 939–946.
- [13] B. J. Reich, "Spatiotemporal quantile regression for detecting distributional changes in environmental processes," *Journal of the Royal Statistical Society: Series C (Applied Statistics)*, vol. 61, no. 4, pp. 535–553, 2012, eprint: <https://rss.onlinelibrary.wiley.com/doi/pdf/10.1111/j.1467-9876.2011.01025.x>.
- [14] C. E. Rasmussen and C. K. I. Williams, *Gaussian Processes for Machine Learning*. MIT press, 2006, iSSN: 0129-0657.
- [15] G. A. Hollinger and G. S. Sukhatme, "Sampling-based robotic information gathering algorithms," *The International Journal of Robotics Research*, vol. 33, no. 9, pp. 1271–1287, 2014.
- [16] R. J. Hyndman and Y. Fan, "Sample Quantiles in Statistical Packages," *The American Statistician*, vol. 50, no. 4, pp. 361–365, 1996, publisher: [American Statistical Association, Taylor & Francis, Ltd.].
- [17] R. Wilcoxon, *Introduction to Robust Estimation and Hypothesis Testing (Third Edition)*, 3rd ed., ser. Statistical Modeling and Decision Science. Boston: Academic Press, 2012.
- [18] J. S. Maritz and R. G. Jarrett, "A Note on Estimating the Variance of the Sample Median," *Journal of the American Statistical Association*, vol. 73, no. 361, pp. 194–196, Mar. 1978.
- [19] P.-T. De Boer, D. P. Kroese, S. Mannor, and R. Y. Rubinstein, "A tutorial on the cross-entropy method," *Annals of operations research*, vol. 134, no. 1, pp. 19–67, 2005.
- [20] S. Kirkpatrick, C. D. Gelatt Jr, and M. P. Vecchi, "Optimization by Simulated Annealing," in *Readings in Computer Vision*. Elsevier, 1987, pp. 606–615.
- [21] J. Snoek, H. Larochelle, and R. P. Adams, "Practical bayesian optimization of machine learning algorithms," in *Advances in Neural Information Processing Systems*, F. Pereira, C. J. C. Burges, L. Bottou, and K. Q. Weinberger, Eds., vol. 25. Curran Associates, Inc., 2012.
- [22] D. R. Jones, M. Schonlau, and W. J. Welch, "Efficient Global Optimization of Expensive Black-Box Functions," *Journal of Global Optimization*, vol. 13, no. 4, pp. 455–492, Dec. 1998.
- [23] C. Qin, D. Klabjan, and D. Russo, "Improving the expected improvement algorithm," in *Proceedings of the 31st International Conference on Neural Information Processing Systems*, ser. NIPS'17. Red Hook, NY, USA: Curran Associates Inc., 2017, p. 5387–5397.
- [24] D. Silver and J. Veness, "Monte-Carlo Planning in Large POMDPs," in *Advances in Neural Information Processing Systems*, J. Lafferty, C. Williams, J. Shawe-Taylor, R. Zemel, and A. Culotta, Eds., vol. 23. Curran Associates, Inc., 2010.
- [25] C. Denniston, A. Kumaraguru, and G. S. Sukhatme, "Comparison of Path Planning Approaches for Harmful Algal Bloom Monitoring," in *OCEANS 2019 MTS/IEEE SEATTLE*, Oct. 2019, pp. 1–9, iSSN: 0197-7385.